










Cite this: DOI: 10.1039/d1gc01777b

On the chemical interactions of the biomass processing agents γ -valerolactone (GVL) and *N*-methylmorpholine-*N*-oxide (NMMO)[†]

Paul Jusner, ^a Markus Bacher, ^a Hubert Hettegger, ^a Huy Quang Lê, ^b
Antje Potthast, ^a Herbert Sixta ^b and Thomas Rosenau ^{*a}

In new biorefinery processes, NMMO/water is used for the pre-treatment of biomass to increase the efficiency of subsequent digestion processes, while GVL/water is used for “organosolv” fractionation of biomass. The combination of both methods, GVL digestion after pre-activation by NMMO, appears to be reasonable, but has not been successful. In the present study, we examine the reason for this failure and investigate the chemical processes in the ternary system NMMO/GVL/water and in the quaternary system NMMO/GVL/water/“biomass”. The consumption kinetics of NMMO and GVL at different temperatures, water contents and NMMO/GVL ratios were recorded. The respective degradation and reaction products were identified for the first time, by combining nuclear magnetic resonance (NMR) spectroscopy, and gas chromatography – mass spectrometry (GC-MS) techniques and synthesis of authentic compounds for comparison. Decomposition products of NMMO and GVL on their own as well as reaction products of both components together (α -morpholinomethyl-GVL (**7**), α -methylene-GVL (**8**), and 4-hydroxyvaleric acid morpholide (**13**)) were observed among the main degradation products. At temperatures of 150 °C and at a water content <10% (or 180 °C and 30%, respectively), the contained NMMO was autocatalytically decomposed in highly exothermic reactions, and explosive processes occurred which caused complete charring of the reaction mixture. At higher water contents, the system remained stable, but NMMO was still completely degraded and GVL was consumed to a significant extent. While the biomass component cellulose was largely unreactive, lignin was the main culprit that caused degradation reactions in the system. The formation of NMM (**5**) from NMMO and the resulting ring opening of GVL to 4-hydroxyvaleric acid (**3**), which is immediately oxidized by NMMO to levulinic acid (**4**), were the initial reactions that triggered the subsequent, more complex decomposition pathways. The chemical structures of all degradation products were fully analytically confirmed. Due to the instability of the NMMO/GVL system, the combination of NMMO biomass pre-treatment and GVL biomass digestion is prohibited, unless a careful removal of NMMO is carried out beforehand. Besides these practical conclusions with regard to biomass processing in biorefineries, the present study provides hopefully helpful insights into the chemistry of NMMO and GVL and the underlying reaction mechanisms.

Received 19th May 2021,
Accepted 25th June 2021

DOI: 10.1039/d1gc01777b

rsc.li/greenchem

Introduction

N-Methylmorpholine-*N*-oxide monohydrate (NMMO, **2**) is the solvent used in the industrial production of cellulosic fibres

according to the Lyocell technology, which is one of the most environmentally benign industrial fibre-making processes developed. NMMO is fully biodegradable¹ and recyclable to more than 99% in the industrial setting.²

NMMO, theoretically, dissolves cellulose in a merely physical process – the strong N–O dipoles³ break the complex hydrogen bond network of cellulose and establish solvent–solute hydrogen bonds, effecting cellulose dissolution. Practically, NMMO tends to react with several chemical agents: the system NMMO/water/cellulose involves complex homolytic (radical) and heterolytic (ionic) degradation reactions,⁴ which – in the worst case – can cause autocatalytic degradation⁵ of the solvent with uncontrollable exothermic reactions. However,

^aUniversity of Natural Resources and Life Sciences Vienna (BOKU),
Department of Chemistry, Institute of Chemistry of Renewable Resources,
Konrad Lorenz-Straße 24, 3430 Tulln an der Donau, Austria.
E-mail: thomas.rosenau@boku.ac.at

^bAalto University, Department of Bioproducts and Biosystems,
School of Chemical Engineering, Vuorimiehentie 1, 02150 Espoo, Finland

[†]Electronic supplementary information (ESI) available. See DOI: 10.1039/d1gc01777b

the use of stabilizers nowadays allows running the industrial applications safely and reliably.⁶

NMMO, as the most widely used amine *N*-oxide oxidant, is frequently employed in chemical synthesis,⁷ mostly as a direct, primary oxidant⁸ or as a secondary oxidant in transition metal-catalysed oxygenations,⁹ as the intermediate to effect stabilization of *ortho*-quinone methides or *N*-dealkylation,¹⁰ for the production of metal nanoparticles,¹¹ or many other reactions, so that reflections on the manifold aspects of NMMO chemistry would go far beyond the scope of this article.

More recently, NMMO has got into the focus of usage attempts as an effective and environmentally compatible auxiliary in the pretreatment of cellulose¹² and lignocellulosic biomass¹³ to facilitate subsequent enzymatic hydrolysis of the polysaccharides contained. NMMO in general closely interacts with water¹⁴ and forms two stable hydrates, a monohydrate (NMMO·H₂O) and a semisquihydrate (NMMO·2.5H₂O). Pretreatment of biomass is carried out in rather concentrated aqueous NMMO solutions which mostly contain 50% or 85% NMMO.

NMMO-pretreated biomass was shown to react faster and to give higher monosaccharide yields upon enzymatic hydrolysis than non-treated biomass.¹⁵ This was attributed to increased accessibility and amorphicity (*i.e.*, decreased crystallinity) of the cellulose after the NMMO pretreatment.¹⁶ The good results of enzymatic cellulose hydrolysis of NMMO-pretreated cotton linters and/or wood (oak, spruce) were attributed to decreased cellulose crystallinity, partial transformation of cellulose I to cellulose II, and an increased capacity of the cellulosic substrate to adsorb the enzymes.^{15c,16a,17} NMMO is considered to widen the lignocellulose structure, swell its microfibrils, and decrease its overall recalcitrance while at the same time maintaining an almost unchanged chemical composition.^{17,18} This effect was similar for wood and non-woody biomass: in all cases the composition was apparently influenced only to a little extent. The composition of rice straw, wheat straw, and corn husks as well as oil palm empty fruit bunches did not change significantly even after prolonged treatments with NMMO for over 10 h.¹⁹

Generally, the yield of enzymatic hydrolysis of polysaccharides in biomass was boosted by NMMO-pretreatment, increasing not only the yield of cellulose-derived glucose, but also the outcome of hemicellulose-derived monosaccharides, such as xylose, glucose and mannose during enzymatic hydrolysis,²⁰ and the effect on methane/biogas yield was similarly positive.²¹ The big advantage, as suggested in the pertinent papers, is that NMMO has no inhibitory effect on the enzymes used, which – in combination with the good biodegradability of NMMO – eliminates the need for extensive washing to remove residual NMMO from the pretreated biomass, as NMMO carry-overs would neither pose an ecological nor a major economic problem.²²

Unlike synthetic NMMO, the cyclic ester γ -valerolactone (GVL, **1**) is a natural substance, occurring as a volatile flavour constituent in many products, such as barley, coffee, cocoa, mango, honey, peach, or mushrooms.²³ GVL has been widely

applied as a food flavour enhancer,²⁴ a perfume component²⁵ or a solvent for lacquer, insecticides, and adhesives.²⁶ GVL is produced from carbohydrate sources *via* levulinic acid,²⁷ which is hydrogenated under heterogeneous catalysis conditions. GVL and its properties comply with Green Chemistry principles for solvents (low volatility, low toxicity, no malodour, and stability under pH-neutral storage conditions),²⁸ which promoted the recent renaissance of GVL-related research activities. Since the first revival of interest led by Horváth *et al.* in 2007,²⁹ GVL has almost been hyped as a green solvent for a variety of chemical and biomass conversion processes.

The most straight-forward production approach for GVL is the synthesis from carbohydrate sources, such as fructose,³⁰ cellulose³¹ or biomass³² in aqueous media, which effectively minimizes the costs for GVL separation and purification. Alternatively, pioneered by Dumesic *et al.*,³³ bio-chemicals, such as lignin monomers, monomeric carbohydrates, organic acids and platform furan compounds, were produced from carbohydrate sources or biomass in aqueous solutions of GVL.³⁴ The apparent activation energies of hydrolysis reactions were lower in GVL than under conventional conditions, allowing for low-temperature operation. Besides this, furfural degradation reactions (to humins) were suppressed in GVL, thus increasing the product yield and allowing the use of solid catalysts with lower risk of deactivation.³⁵

GVL has been widely employed in the thermochemical pretreatment of biomass for improving enzymatic activities in the production of biofuels.³⁶ Full biorefinery concepts based on GVL pulping have been developed by Sixta *et al.*³⁷ and Dumesic *et al.*³⁸ to produce dissolving pulp and other value-added products from lignocellulosic biomass.^{24–26} Luterbacher *et al.* introduced a lignin-first biorefinery concept based on the aldehyde-stabilized GVL treatment of biomass to produce less condensed lignin with a high content of native linkages, which was more susceptible to depolymerization to monoaromatic compounds than other technical lignins.³⁹

Given the advantages of NMMO pretreatment and GVL biomass fractionation, each on its own, it was logical, at least at first sight, to attempt a combination of the two to check for possible synergistic, beneficial effects.⁴⁰ On the one hand, the NMMO pretreatment was expected to reduce the process temperature, and thus the energy input of the subsequent GVL fractionation step, and on the other hand, the GVL fractionation would open utilization ways for NMMO-pretreated biomass other than just enzymatic saccharification or biogas production, for instance direct material utilization of the cellulose and lignin fractions.

A combination of both compounds, of course, raises the issue of whether the NMMO system and the GVL system are chemically compatible or not. This is especially important as NMMO residues from the pretreatment step are usually not meticulously removed (see above) so that appreciable amounts of NMMO are carried forward into the GVL biomass fractionation. While both NMMO pretreatment and GVL fractionation of biomass have been shown to be fairly devoid of degradation

reactions and byproduct formation, this cannot necessarily be assumed for the combination of the two agents (see the ESI† for known incidents).

Previous research has demonstrated how important and surprising the chemistry of byproducts and side reactions in allegedly fully physical processes during biomass processing can be. This starts with the formation of highly reactive agents, such as keteniminium ions from the cellulose solvent *N,N*-dimethylacetamide/LiCl⁴¹ or methyl(methylene)sulfonium ylide from the cellulose derivatizing system DMSO/phenylisocyanate⁴² that degrade cellulose and, if not avoided, render respective analytical methods highly inaccurate. Such research also includes examples of high economic and ecological relevance, such as chromophore formation in cellulose and the associated bleaching requirements⁴³ or the derivatization of cellulose by degradation products of allegedly inert ionic liquids,⁴⁴ and even touches upon aspects of work safety and health, such as the avoidance of the formation of *N*-(methylene)morpholinium ions in the industrial production of Lyocell fibres.^{4,5} From such former studies we were able to draw on experience with by-product formation and complex reaction systems involving biomass components, from which we hoped to benefit methodologically also for the present work. The aspects of the chemical compatibility of NMMO biomass pretreatment and GVL biomass fractionation, in particular the questions which side reactions occur and which by-products are formed, were the incentives of this study.

Experimental section

General

All chemicals were purchased from commercial suppliers and were of the highest purity available. Solvents of highest purity available were used for all extractions and workup procedures. Distilled water was used throughout. Anhydrous NMMO was recrystallized twice from acetone before use. TLC was performed using Merck silica gel 60 F₂₅₄ pre-coated plates. Flash chromatography was performed on Baker silica gel (40 µm particle size). All products were purified to homogeneity (TLC/GC analysis).

Beech sawdust was produced by milling of bark-free, air-dried beech wood (Retsch lab mill, Haan, Germany); only particles with sizes below 150 µm were used; the chemical composition of the wood was as follows: 47.9% cellulose (glucose), 21.2% hemicelluloses (15.8% xylose and 5.4% other monosaccharides), 26.2% lignin, 1.1% extractives and 0.3% ash. Commercially available cellulose (Avicel PH-101 microcrystalline cellulose, Sigma-Aldrich) was used, along with hemicellulose (beech xylan) and lignin (beech and spruce milled wood lignin) available from earlier work.⁴⁵

Analysis and compound identification by nuclear magnetic resonance (NMR) spectroscopy

For NMR analysis, a Bruker Avance II 400 instrument (¹H resonance at 400.13 MHz, ¹³C resonance at 100.62 MHz) with a

5 mm broadband probe head (BBFO) equipped with a z-gradient with standard Bruker pulse programs was used. Data were collected with 32k data points and apodized with a Gaussian window function (GB = 0.3) prior to Fourier transformation. A 2.5 s acquisition time and a 1 s relaxation delay were used. A Bruker TopSpin 3.5 spectrometer was used for the acquisition and processing of the NMR data. Spectra were recorded in CDCl₃ in the case of isolated compounds (either from degradation mixtures or authentic samples for comparison), or in DMSO-d₆ for determination of the composition of the reaction mixtures. Chemical shifts, relative to TMS as an internal standard, are given in δ ppm values, and coupling constants in Hz. ¹³C peaks were assigned by means of APT, HSQC and HMBC spectra.

GC-MS analysis (liquid phase)

To a 0.5 mL aliquot of the sample in dichloromethane 200 µL of anhydrous pyridine containing 1.5 mg mL⁻¹ 4-dimethylaminopyridine (DMAP) and 200 µL *N,O*-bis(trimethylsilyl)trifluoroacetamide (BSTFA) containing 10% trimethylchlorosilane (TMCS) were added. The mixture was heated for 2 h at 70 °C and allowed to cool to room temperature. The sample was diluted to 1.00 mL with dichloromethane and an aliquot of 0.2 µL was injected.⁴⁶ The GC-MS analysis was carried out on an Agilent 7890A gas chromatograph with an Agilent 5975C triple axis mass selective detector (MSD). Column: DB5-ms (30 m × 0.25 mm i.d., 0.25 µm film thickness; J&W Scientific, Folsom, CA, USA). The MMI multi-mode inlet was operated under the following conditions: splitless injection, constant column flow: 0.9 mL min⁻¹ with helium as the carrier gas, purge flow: 15.0 mL min⁻¹ (0.75 min); injector: constant *T* = 260 °C. Temperature profile: 50 °C (2 min), then 5 °C min⁻¹ to 280 °C (20 min). MS detection: EI mode, 70 eV ionization energy, 1.13 × 10⁻⁷ Pa, ion source temperature: 230 °C, quadrupole: 150 °C, transfer line: 280 °C. Data acquisition: scan from 45 to 950 *m/z*. Injection: 0.2 µL, CTC-PALxt autosampler, Chronos software v.3.5 (Axel Semrau, Spockhövel, Germany). The NIST/Wiley 2008 database was used for compound identification.

Headspace GC-MS analysis (gas phase)

GC-MS analysis was carried out on an Agilent 6890 gas chromatograph with an Agilent 5975C mass selective detector (MSD). Column: VF-WAXms (30 m × 0.25 mm i.d., 0.25 µm film thickness; J&W Scientific, Folsom, CA, USA). The MMI multi-mode inlet was operated under the following conditions: splitless injection, constant column flow: 0.9 mL min⁻¹ with helium as the carrier gas, purge flow: 15.0 mL min⁻¹ (0.75 min); injector: constant at 250 °C. Temperature profile: 40 °C (2 min), then 8 °C min⁻¹ to 250 °C (6 min). MS detection: EI mode, 70 eV ionization energy, 1.13 × 10⁻⁷ Pa, ion source temperature: 230 °C, quadrupole: 150 °C, transfer line: 280 °C. Data acquisition: scan from 45 to 500 *m/z*. Injection: 3 mL headspace, Agilent 7694 headspace sampler, 3 min equilibration at 50 °C, vial pressurization time: 0.2 min, loop fill time: 0.18 min, loop equilibration time: 0.05 min, injection

time: 1 min. The NIST/Wiley 2008 database was used to support compound identification.

General procedure for studies of the chemical integrity in the ternary system GVL/NMMO/water and the quaternary system GVL/NMMO/water/biomass

Experiments on reactions in the GVL- and NMMO-containing reaction systems were performed in 100 mL stainless steel bombs with inner PTFE coating equipped with a magnetic stirrer and a valve that allowed withdrawing gaseous or liquid samples. The procedure was adapted from previous work.^{37c} The reactors were inserted into an aluminium block system (2mag AG Munich; Germany) with internal electrical heating and 15 separately stirrable wells (70 mm i.d., 80 mm deep) so that 15 reactions could be carried out in parallel. The heating block allowed controlled rapid heating (250 °C min⁻¹) and a temperature accuracy of ± 2 °C. Cooling was performed by quickly immersing the reactors in a water bath which allowed reaching the target temperature (r.t.) within less than 15 s.

CAUTION! NMMO containing mixtures, especially at temperatures >100 °C, may undergo spontaneous, uncontrollable degradation reactions and explosive decomposition! Appropriate pressure-proof reactors, working in a hood, and appropriate protection wear are absolutely necessary! Minimizing reagent amounts is recommended!

The reactors were filled to a volume of maximum 50 mL with the ratios of the components of the reaction mixture being set according to Fig. 1–4 (see the corresponding text). After fast heating within less than 1 min, the target temperature (100, 125, 150 or 180 °C, see Fig. 1–4) was kept for 2 h. The reactors were quickly cooled to r.t. as described above and opened. In all cases where charring of the content occurred as a result of autocatalytic NMMO degradation, the black, intractable precipitate was discarded. In some cases, the gas phase was withdrawn through the sample valve and analysed by headspace GC-MS. Solids from biomass were filtered off through a sintered glass frit. A 200 μ L aliquot of the liquid phase was dissolved in 400 μ L of DMSO-*d*₆ and analysed by ¹H NMR to determine the loss of GVL and NMMO (see above).

Isolation of degradation products was performed only in cases where NMR indicated extensive degradation of NMMO and/or GVL and formation of by-products, otherwise the amounts isolated would have been too small for a reliable identification. The liquid phase was poured into a saturated aqueous NaCl solution (100 mL, pH = 4 set with conc. HCl), stirred vigorously for 1 min and extracted with dichloromethane (3 \times 20 mL). The organic extracts were combined. The aqueous phase was brought to pH 10 (2 M NaOH) and extracted again with dichloromethane (3 \times 20 mL). The aqueous phase was discarded and all organic extracts (from both the acidic and alkaline aqueous phases) were combined, washed with brine (20 mL) and dried over MgSO₄. Evaporation of the solvent *in vacuo* was performed at r.t. in order not to lose highly volatile components. An aliquot of the residue was dissolved in CDCl₃ for NMR and GC-MS analysis. The bulk of the residue was dissolved in chloroform and subjected to

column chromatography on silica gel with an ethyl acetate/toluene (v/v = 4 : 1) eluant. The isolated components were analysed by NMR and GC-MS (see above). The identity of the reported components was in all cases confirmed additionally by comparison with authentic samples, which were either commercially available or independently synthesized.

Analytical characterization of GVL- and NMMO-degradation products

Levulinic acid (4). ¹H NMR (CDCl₃): δ 2.12 (s, 3H, 5-CH₃), 2.54 (t, *J* = 6.1 Hz, 2H, 2-CH₂), 2.69 ppm (t, *J* = 6.1 Hz, 2H, 3-CH₂). ¹³C NMR: δ 27.6 (2-CH₂), 29.5 (5-CH₃), 37.5 (3-CH₂), 178.3 (1-CO), 207.0 ppm (4-CO). Anal. calcd for C₅H₈O₃: C 51.72, H 6.94; found C 51.76, H 6.99.

N-Methylmorpholine (5). ¹H NMR (CDCl₃): δ 2.27 (s, 3H, N-CH₃), 2.39 (t, 4H, N-CH₂), 3.70 (t, 4H, O-CH₂). ¹³C NMR: δ 43.7 (N-Me), 53.8 (d.i.), 64.1 ppm (d.i.). Anal. calcd for C₅H₁₁NO: C 59.37, H 10.96, N 13.85; found: n.d.

5-Methyl-3-(morpholinomethyl)dihydrofuran-2(3H)-one, α -morpholinomethyl- γ -valerolactone (7). ¹H NMR (CDCl₃): δ 1.37 (d, 3H, CH₃), 2.12 (m, 1H, 4-CH_A), 2.54–2.62 (m, 2H, 4-CH_B, 3-CH-CH_A), 2.72 (m, 4H, N-CH₂), 2.91 (m, 1H, 3-CH-CH_B), 3.62 (m, 4H, O-CH₂), 4.54 ppm (sext, 1H, 5-CH). ¹³C NMR: δ 20.8 (CH₃), 34.1 (4-CH₂), 45.0 (3-CH), 45.6 (d.i., N-CH₂), 49.8 (3-CH-CH₂), 65.9 (d.i., O-CH₂), 75.0 (5-CH), 175.9 ppm (1-CO). Anal. calcd for C₁₀H₁₇NO₃: C 60.28, H 8.60, N 7.03; found C 60.19, H 6.72, N 7.14.

5-Methyl-3-methylenedihydrofuran-2(3H)-one, α -methylene- γ -valerolactone (8). ¹H NMR (CDCl₃): δ 1.39 (m, 3H, CH₃), 2.51 (ddt, *J* = 17.0, 6.0, 2.9 Hz, 1H, 4-CH_A), 3.07 (ddt, *J* = 17.0, 7.6, 2.6 Hz, 1H, 4-CH_B), 4.64 (m, 1H, 5-CH), 5.60 (t, *J* = 2.6 Hz, 1H, methylene-H_A), 6.18 ppm (t, *J* = 2.9 Hz, 1H, methylene-H_B). ¹³C NMR: δ 21.9 (CH₃), 35.0 (4-CH₂), 73.9 (5-CH), 121.9 (methylene-CH₂), 134.8 (2-C), 170.3 ppm (1-CO). Anal. calcd for C₆H₈O₂: C 64.27, H 7.19; found C 64.32, H 7.26.

Morpholine (9). ¹H NMR (CDCl₃): δ 1.73 (s, b, 1H, NH), 2.87 (m, 4H, N-CH₂), 3.68 ppm (m, 4H, O-CH₂). ¹³C NMR: δ 46.4 (d.i.), 64.1 ppm (d.i.). Anal. calcd for C₄H₉NO: C 55.15, H 10.41, N 16.08; found C 55.08, H 10.62, N 15.96.

5-Methylfuran-2(3H)-one, α -angelicalactone (10). ¹H NMR (CDCl₃): δ 1.96 (td, *J* = 2.6, 1.6 Hz, 3H, CH₃), 3.14 (“pent”, *J* = 2.6 Hz, 2H, CH₂), 5.10 ppm (m, CH). ¹³C NMR: δ 13.9 (CH₃), 34.0 (CH₂), 99.0 (CH), 153.2 (C-CH₃), 176.9 ppm (CO). Anal. calcd for C₅H₆O₂: C 61.22, H 6.17; found C 61.34, H 6.03.

3-Pentenoic acid (11). ¹H NMR (CDCl₃): δ 1.70 (ddt, *J* = 6.0, 1.4, 1.4 Hz, 3H, 5-CH₃), 3.06 (dm, *J* = 6.6 Hz, 2H, 2-CH₂), 5.52 (m, 1H, 3-CH), 5.60 ppm (m, 1H, 4-CH). ¹³C NMR: δ 17.9 (5-CH₃), 37.7 (2-CH₂), 121.9 (3-CH), 130.1 (4-CH), 178.9 ppm (1-CO). Anal. calcd for C₅H₈O₂: C 59.98, H 8.05; found C 60.12, H 8.17.

4-Pentenoic acid (12). ¹H NMR (CDCl₃): δ 2.38 (m, 2H, 3-CH₂), 2.47 (m, 2H, 2-CH₂), 5.02 (ddt, *J* = 10.2, 1.5, 1.5 Hz, 1H, 5-CH_A), 5.08 ((ddt, *J* = 17.0, 1.5, 1.5 Hz, 1H, 5-CH_B), 5.83 ppm (ddt, *J* = 17.0, 10.2, 6.3 Hz, 1H, 4-CH). ¹³C NMR: δ 28.4 (3-CH₂), 33.3 (2-CH₂), 115.7 (5-CH₂), 136.2 (4-CH), 179.8 ppm (1-CO). Anal. calcd for C₅H₈O₂: C 59.98, H 8.05; found C 59.87, H 8.07.

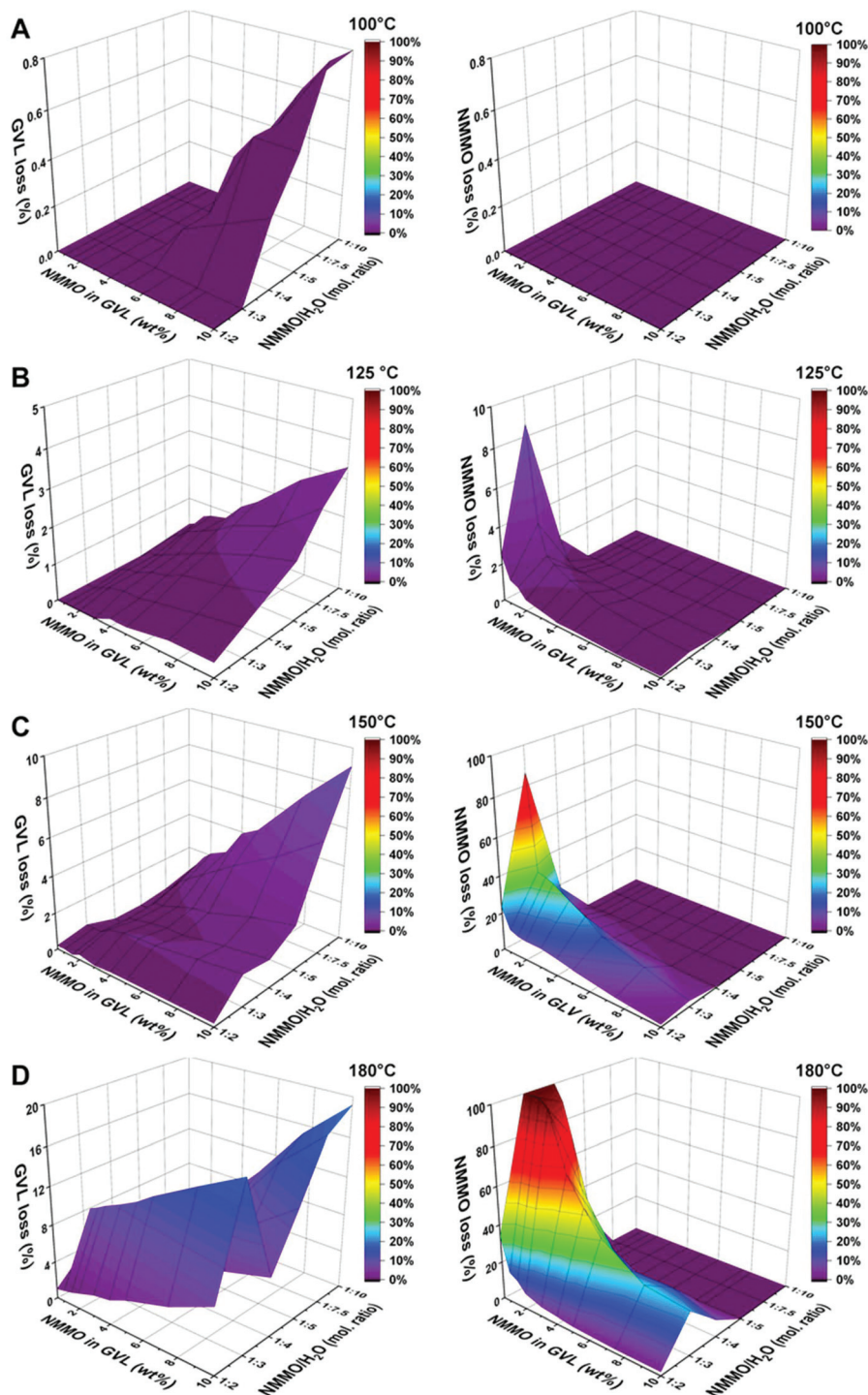


Fig. 1 The ternary system GVL/NMMO/water. Consumption of GVL and NMMO by side reactions (hydrolysis, degradation) at different temperatures covering NMMO contents between 0.5 and 10 mol% relative to GVL and NMMO/water molar ratios between 1: 2 and 1: 10. A: 100 °C, B: 125 °C, C: 150 °C, D: 180 °C. Cf. Fig. 3 for the corresponding quaternary system with an additional biomass component. The numerical values of NMMO and GVL losses, on which the graphical representations are based, are listed in the ESI.†

4-Hydroxyvaleric acid morpholide (13). ^1H NMR (DMSO- d_6): δ 1.07 (d, 3H, CH_3), 1.60 ("q", 2H, $\text{CO-CH}_2\text{-CH}_2$), 2.32 (t, 2H, CO-CH_2), 3.47 (m, 4H, N-CH_2), 3.65 (m, 4H, O-CH_2), 3.68 ppm ("sext", 1H, CH(OH)). ^{13}C NMR: δ 21.2 (CH_3), 28.8

($\text{CO-CH}_2\text{-CH}_2$), 34.1 (CO-CH_2), 45.6 (d.i., N-CH_2), 66.3 (d.i., O-CH_2), 67.0 (CH(OH)), 172.9 ppm (CO). Anal. calcd for $\text{C}_9\text{H}_{17}\text{NO}_3$: C 57.73, H 9.15, N 7.48; found C 57.59, H 9.40, N 7.34.

100 °C	5% NMMO	10% NMMO	15% NMMO	20% NMMO
50:50	😊	😊	😊	😊
60:40	😊	😊	😊	😊
70:30	😊	😊	😊	😊
80:20	😊	😊	😊	😊
90:10	😊	😊	😊	😊
100:0	😊	😊	😊	😊

125 °C	5% NMMO	10% NMMO	15% NMMO	20% NMMO
50:50	😊	😊	😊	😊
60:40	😊	😊	😊	😊
70:30	😊	😊	😊	😊
80:20	😊	😊	😊	😊
90:10	😊	😊	😊	😊
100:0	😞	😞	😞	😞

150 °C	5% NMMO	10% NMMO	15% NMMO	20% NMMO
50:50	😊	😊	😊	😊
60:40	😊	😊	😊	😊
70:30	😊	😊	😊	😊
80:20	😊	😊	😊	😞
90:10	😞	😞	😞	😞
100:0	😞	😞	😞	😞

180 °C	5% NMMO	10% NMMO	15% NMMO	20% NMMO
50:50	😊	😊	😊	😊
60:40	😊	😊	😊	😊
70:30	😊	😞	😞	😞
80:20	😞	😞	😞	😞
90:10	😞	😞	😞	😞
100:0	😞	😞	😞	😞

Fig. 2 Stability of the system GVL/NMMO/water/biomass at different temperatures over 2 h. The first columns of the tables show the GVL/water molar ratios. Complete degradation of the reaction mixture under char formation (red) and stable systems with degradation reactions proceeding, but without any violent effects (green).

Results and discussion

The system GVL/NMMO/water

The interaction of GVL (1) and NMMO (2) depends mainly on the presence of water. This is not only a concentration effect, since the presence of water reduces the effective concentration of the other two components, but is also chemically determined: it has long been known that anhydrous NMMO behaves differently from its monohydrate, which in turn behaves differently from the respective semisquihydrate or aqueous NMMO solutions. The same applies to GVL: in the absence of water and no other co-reactants present, for example, a hydrolysis reaction is evidently impossible. The material safety data sheets (MSDS) of both NMMO and GVL (see the ESI†) do not contain any information about possible incompatibilities of the two compounds.

In a first step, we investigated the interaction of GVL with anhydrous NMMO. These reaction conditions might be less relevant for biomass systems, but have been included for the sake of completeness. An equimolar mixture of GVL and NMMO as well as a mixture in the molar ratio 10:1 was heated at different temperatures (100, 125, 150 and 180 °C) for 2 h and the mixture was analysed with respect to its degradation products. At 100 and 125 °C, no changes in the system were found, at 150 °C there was a slight yellow colouring observed, and at 180 °C a clear yellow discoloration occurred. In none of the cases could degradation or reaction products be isolated or identified. The yellow hue of the solution is due to

the formation of chromophores, which are visible to the naked eye even at very low concentrations (ppb to ppt) but cannot be detected by conventional means such as NMR, HPLC, GC or TLC at the given concentrations. In the absence of water and other reaction partners, the binary system GVL/NMMO can therefore be regarded as largely stable and the two components as inert.

The next step was to investigate the equimolar binary system GVL and NMMO monohydrate, which in principle can also be regarded as an equimolar, ternary mixture of the three components GVL, NMMO and water. Again, an additional mixture in a ratio of 10:1 was also used, *i.e.* the three species were present in a molar ratio of GVL/NMMO/H₂O = 10:1:1. Interestingly, the results were very similar to those obtained using anhydrous NMMO. At none of the four temperatures tested (see above) a detectable chemical reaction occurred. In contrast to anhydrous NMMO, the mixture remained almost colourless even at 150 and 180 °C. This result was unexpected insofar as one would assume an increase in GVL hydrolysis due to the water present in NMMO monohydrate, especially at higher temperatures. However, it is known that in mixtures of NMMO, due to the high polarity of the N–O bond, the water remains fixed to the NMMO *via* strong hydrogen bonds and is not a mobile species. Obviously, such water is not available for the hydrolysis of GVL. The lower yellowing due to traces of chromophores can be explained by the lower oxidation power of NMMO monohydrate compared to anhydrous NMMO. In the absence of any co-reactants, the GVL/NMMO

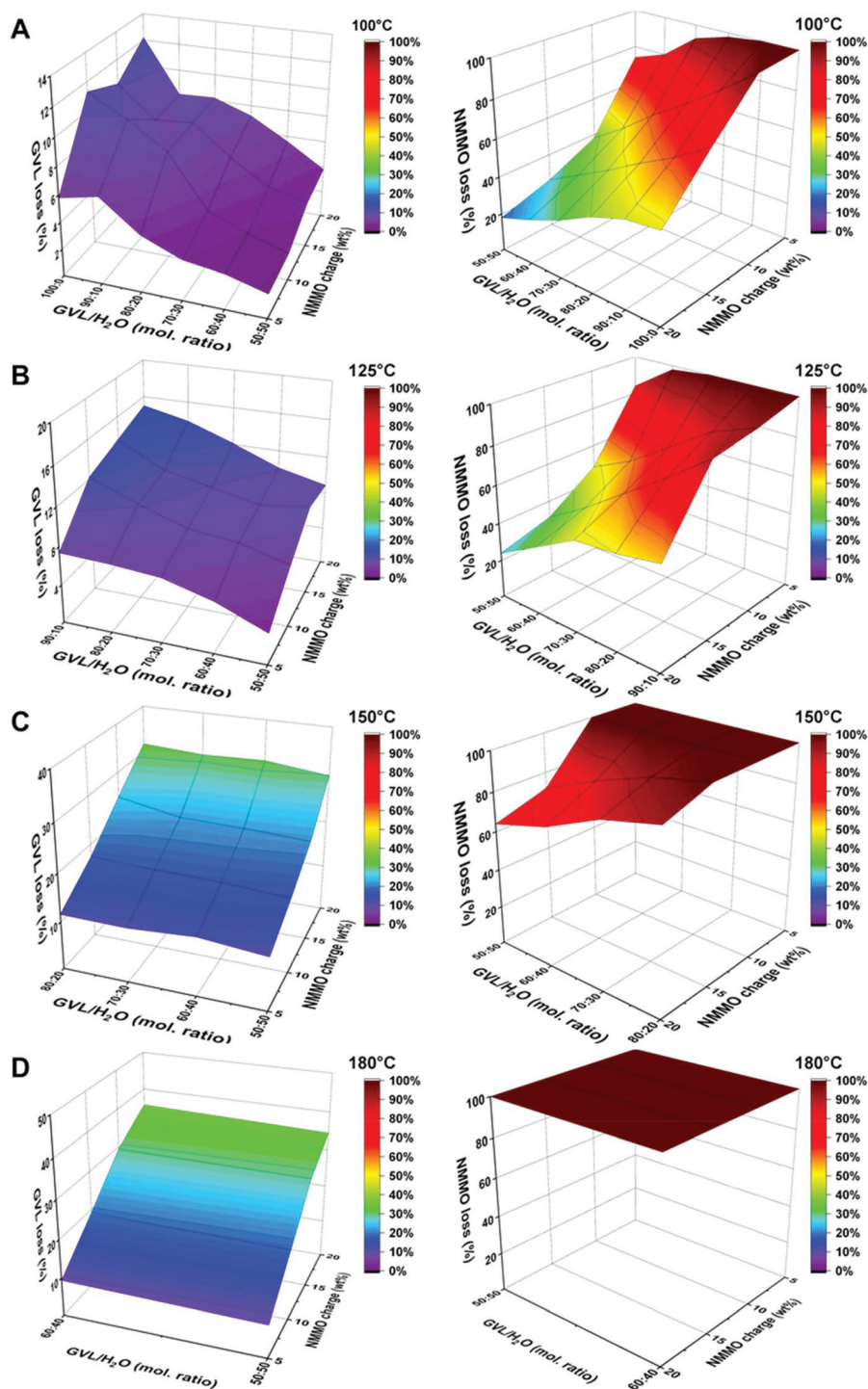


Fig. 3 The quaternary system GVL/NMMO/water/biomass with 10 wt% biomass relative to the GVL/water phase. Consumption of GVL and NMMO by side reactions (hydrolysis, degradation) at different temperatures covering NMMO contents of 5, 10, 15 and 20% relative to biomass and molar GVL/water ratios between 100 : 0 and 50 : 50. A: 100 °C, B: 125 °C, C: 150 °C, D: 180 °C. Cf. Fig. 1 for the corresponding ternary system without the biomass component. The numerical values of NMMO and GVL losses, on which the graphical representations are based, are listed in the ESI.†

monohydrate system is stable and its two components are inert.

To further study the GVL/NMMO/water mixture exhaustively throughout the whole space of this ternary system, with all

possible ratios between the three components, might be of theoretical interest, but is not relevant in practice. If biomass is activated by NMMO treatment, the NMMO carryover into the GVL system is typically in the low percent range relative to

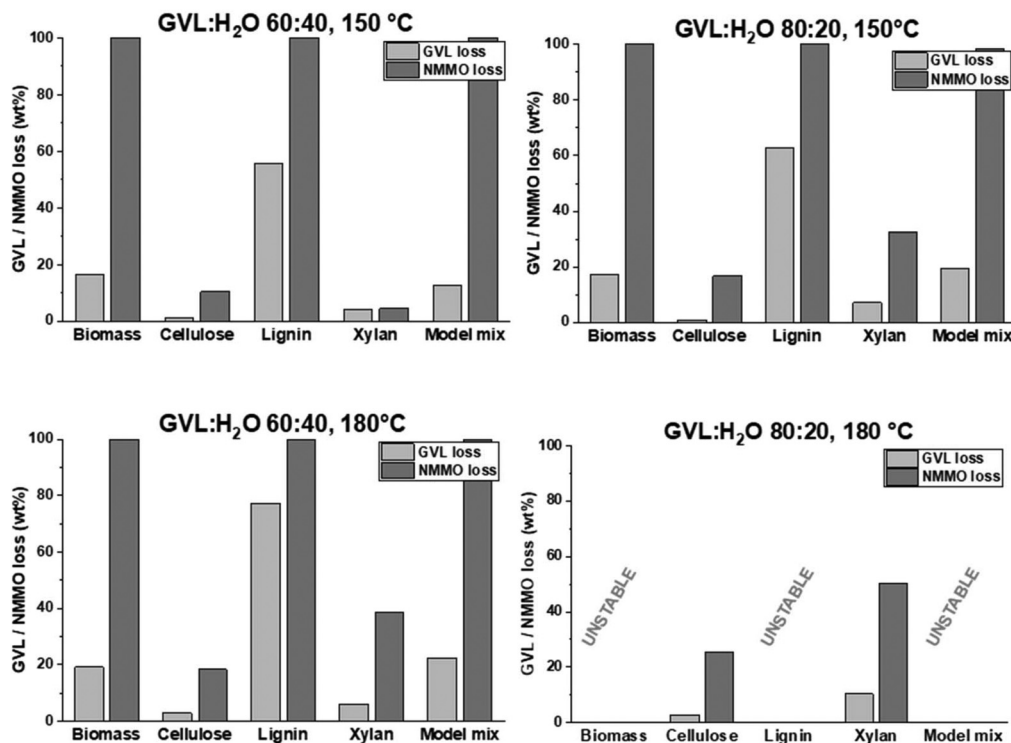


Fig. 4 The quaternary system GVL/NMMO/water/biomass component (cellulose, lignin, xylan) with 10 wt% biomass component relative to the GVL/water phase. Consumption of GVL and NMMO by side reactions (hydrolysis, degradation) at different temperatures and a NMMO content of 10% (relative to biomass component), molar GVL/water ratios = 90 : 10 and 60 : 40. Cf. Fig. 1 for the corresponding ternary system without the biomass component. The values for biomass (as a "single chemical component"), taken from Fig. 3, are shown for comparison. The numerical values of NMMO and GVL losses, on which the graphical representations are based, are listed in the ESI.†

GVL. In our experiments we covered the range of 1–10 wt% NMMO with respect to GVL. For biomass pretreatment, usually a 50 wt% solution of NMMO in water is used, which corresponds to a molar NMMO/water ratio of 1 : 6.5. Ratios between 1 : 2 and 1 : 10 were covered in our experiments. We thus determined the ternary compositional space with NMMO contents of 0.5, 1, 1.5, 2, 3, 4, 5, 7.5 and 10 wt% relative to GVL, and molar NMMO/water ratios of 1 : 2, 1 : 3, 1 : 4, 1 : 5, 1 : 7.5, and 1 : 10. The mixtures were subjected to heating for 2 h at four different temperatures (100, 125, 150 and 180 °C) in a closed pressure vial, before they were analysed for decomposition or degradation reactions. 180 °C is a typical temperature for non-catalysed GVL-organosolv treatments of biomass. The ratio of the components can be easily determined by ¹H NMR based on the integrals, while quantitation – and thus determination of the remaining content relative to the starting concentration – is achieved by ¹H NMR relative to an internal standard (pivalic acid, Me₃C–COOH, δ = 1.23 ppm). For each temperature level, this approach resulted in 63 mixture compositions, for each of which the chemical integrity of the contained species had to be investigated. We first focused on the consumption of the starting components, without identification of the degradation products. The results of the experiments are shown graphically in Fig. 1. While the x-axis and

y-axis give the content of NMMO in GVL (wt%) and the molar ratio NMMO/H₂O, the z-axis shows the loss of GVL (in %) and the loss of NMMO (in %). The numerical yield values are given in the ESI.†

At a temperature of 100 °C, NMMO was inert at all water contents: no degradation whatsoever was observed. At the highest water contents (5% NMMO and above, water/NMMO = 4 : 1 and above), some GVL hydrolysis was noticeable, but remained well below approx. 3%. At higher temperatures, the degradation tendency for both GVL and NMMO increased, because evidently the decomposition reactions proceeded faster with increasing temperatures. It was obvious that the NMMO degradation at a NMMO/water ratio of 1 : 2 was relatively small, had a maximum at a ratio of 1 : 3, and decreased at a ratio of 1 : 4. This effect became more pronounced when going from 125 to 150 and 180 °C. At an NMMO/water ratio above 1 : 4, no NMMO was consumed, not even at 180 °C. The lower reactivity of the 1 : 2 mixture compared to the 1 : 3 counterpart can again be explained by the ability of NMMO to bind up to 2.5 equivalents of water in stable structures. NMMO forms two stable hydrates, a monohydrate NMMO·H₂O and a semisessquihydrate NMMO·2.5H₂O (or better 2NMMO·5H₂O); water at NMMO/water ratios below 2.5 would be tightly bound and less free to react otherwise. At a

ratio of 1 : 3, little free, not NMMO-bound water is present. With increasing NMMO/water ratio, the amount of free water increases and the oxidation power of NMMO in turn decreases significantly. This effect is well known from the realm of synthetic organic chemistry, where NMMO is either applied as an oxidant in its anhydrous form or as the respective monohydrate. The observed “protective effect” of water on NMMO in the GVL system at water/NMMO ratios of 4 : 1 and above is also due to this dilution effect: the excess of water increasingly deactivates the NMMO and decreases its reactivity as an oxidant so that it remains unchanged at large water ratios, despite the high reaction temperatures. At 125 °C maximum consumption of NMMO was approx. 8% (at 0.5% NMMO and a NMMO/water ratio of 1 : 3), while it rose to 86% at 150 °C (at the same composition). At 180 °C, NMMO degradation was complete, even over a relatively large composition range (at NMMO contents between 0.5 and 5%, NMMO/water ratios 1 : 3 and 1 : 4).

The fact that NMMO and NMMO monohydrate were inert towards GVL, also at higher temperatures, as established above, seemed to deny the observed NMMO degradation at higher water contents at a first glance. But as soon as one considers that the main co-reactant of NMMO is not GVL itself, but its reaction (hydrolysis) product(s) with water, this contradiction disappears, and the observed shapes of the ternary systems in Fig. 1 become very clear.

First, we see that the consumption of GVL by hydrolysis is increasing with an increasing amount of free water. The water amount can increase either by a higher NMMO content with a fixed NMMO/water ratio or by an increasing NMMO/water ratio at a certain NMMO level in GVL. Generally, more water in the system promotes GVL hydrolysis, but even at an NMMO content of 10% at an NMMO/water ratio of 1 : 10 – in this case water and GVL are present in equimolar amounts – only 19% of GVL is hydrolysed. The high stability of the cyclic, 5-membered lactone compared to its open-chain γ -hydroxyacid counterpart is mainly due to entropic reasons that favour the cyclic structure, and the 5-membered ring in particular. Second, it was obvious that NMMO oxidation of GVL hydrolysis products occurred only when the oxidation power of NMMO was not diminished by too high water contents, *i.e.* at NMMO/water ratios below 1 : 5. Thus, water in the system had an ambivalent effect: on the one hand, increasing water amounts

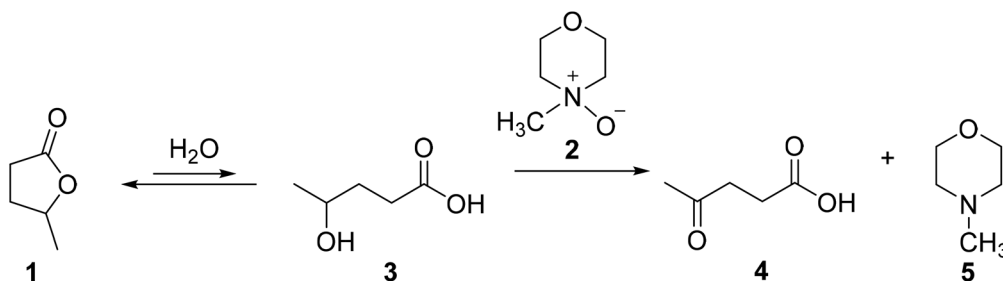
promoted GVL consumption by hydrolysis, and on the other hand, higher concentrations deactivated NMMO and decreased its reactivity as an oxidant. At lower water contents, only small amounts of GVL hydrolysis products are present, but these react readily with NMMO. At higher concentrations, much more GVL hydrolysis products are available in the system, but NMMO is not reactive enough anymore to convert them further.

The reaction products of NMMO with the primary GVL hydrolysis products were evidently able to react with GVL in secondary reactions, because the consumption of GVL showed a local maximum at the NMMO/water ratio of 1 : 3, and then decreased with increasing water amounts to rise again at very high water contents (hydrolysis). This causes the peculiar “bimodal” shapes of the GVL consumption graphs in Fig. 1. The maxima of GVL consumption at the NMMO/water ratio of 1 : 3 coincide with the maxima of NMMO degradation. NMMO reacts with the hydrolysis products of GVL, and the NMMO degradation products, in turn, consume some GVL in addition. The second maximum of GVL consumption at high water contents (high NMMO contents and NMMO/water ratios) originates from GVL hydrolysis, but without further involvement of NMMO.

Degradation products in the system GVL/NMMO/water

This discussion of the chemical processes in the ternary system GVL/NMMO/water must appear oddly theoretical as long as the degradation reactions and products are not specified. The only three degradation products identified are shown in Scheme 1, namely 4-hydroxyvaleric acid (3), *N*-methylmorpholine (NMM, 4) and levulinic acid (5). The compounds were detected at random in all samples and were quantified in the cases where their concentration was highest. No other reaction products were found. The concentrations of the degradation products can be retrieved from Fig. 1 and from the yield tables in the ESI.† The loss in NMMO is equal to the molar amount of levulinic acid (and *N*-methylmorpholine) produced. The loss of GVL corresponds to the amount of 4-hydroxyvaleric acid generated, which in some cases is diminished by the amount of levulinic acid produced by the reaction with NMMO.

This makes the chemical processes in the ternary system very clear. 4-Hydroxyvaleric acid (3) is the hydrolysis product of



Scheme 1 Chemical processes in the system GVL (1)/NMMO (2)/water and chemical structures of the by-products generated: 4-hydroxyvaleric acid (3), levulinic acid (4) and *N*-methylmorpholine (5).

GVL. It is formed as soon as water reacts with GVL, although the equilibrium is far on the side of the more stable lactone. Opposite to GVL, which does not react with NMMO, compound **3** has a secondary hydroxyl group which is readily oxidized by NMMO to give levulinic acid and NMM. As seen in an independent experiment, the reaction between 4-hydroxyvaleric acid and NMMO is complete within less than 20 min at near-quantitative yields, employing equimolar amounts of NMMO monohydrate at 150 °C in GVL as the solvent. The generated NMM is present as the corresponding *N*-methylmorpholinium (ammonium) salts of the respective acids present. In all cases, within the errors of measurement, the sum of levulinic acid and 4-hydroxyvaleric acid corresponded exactly to the loss of GVL, while the concentrations of NMM and levulinic acid in a sample were always the same, in agreement with the processes shown in Scheme 1. When NMM was absent, also no levulinic acid was found, and *vice versa*.

The system GVL/NMMO/water/biomass

It is evident that a mixture of GVL, NMMO, water and biomass is not a quaternary system in the conventional sense: biomass is obviously not a single compound, and even if we neglect its heterogeneity and approximate “biomass” roughly as being one chemical entity with properties averaged from its individual components, screening the whole four-dimensional compositional space of the GVL/NMMO/water/biomass would be utterly challenging.

Fortunately, the practice of biomass valorisation largely limits this compositional space, and only certain concentration ranges are practicable and reasonable. A pretreatment of biomass with NMMO is usually carried out in a way that 5–10% biomass is heated in a mixture of NMMO and water. The process liquor is then washed out with hot water, an organic solvent, such as ethanol, or simply removed by pressing. Typical conditions are treatment times of 1–5 h and temperatures around 100–140 °C. The NMMO/water ratios are typically between 1 : 1 and 1 : 10. The residual content of NMMO in the pretreated biomass is below 5 wt% after washing and about 20 wt% after pressing (relative to wet biomass). The pretreatment has been shown to have no influence on the composition of the biomass, but to increase accessibility to enzymes or pulping chemicals in subsequent saccharification or fractionation steps. Lots of research endeavours have also been dedicated to the question of whether (and if so, how) NMMO influences subsequent saccharification of the polysaccharides or delignification of the biomass.

Fractionation of biomass in GVL is typically performed in GVL/water mixtures of 50–80 wt% GVL, corresponding to molar GVL/water ratios of approx. 1 : 5.5 and lower, at temperatures around 180 °C for 1–3 h. The liquid-to-solid ratio is typically around 3–10 L kg⁻¹. This is followed by separation of solids (mostly cellulose) and process liquor (containing lignin, hemicellulose, extractives, and degradation products) which can be further fractionated and refined.

In accordance with these numbers, we used the following compositions in our tests: GVL/water mass ratios of 50 : 50,

60 : 40, 70 : 30, 80 : 20, 90 : 10 and 100 : 0, and 10% biomass containing 5, 10, 15 and 20% NMMO. As representative biomass samples either milled air-dried wheat straw or milled air-dried beech sawdust was used, as well as isolated biomass components for special experiments (see below). The biomass sample was premixed with the respective amount of NMMO, then mixed with the GVL/water mixture and heated to the corresponding reaction temperature (100, 125, 150 or 180 °C as already used in the experiments without biomass) in a sealed pressure vial. An actual “pretreatment” step with NMMO/water was not carried out, but the solid biomass/NMMO premix was directly added to the liquid GVL/water phase. The amount of water contained in the biomass/NMMO sample is very small compared to the amount of water in the GVL/water phase, and was therefore considered to be negligible. Therefore, only NMMO was used for the premix with biomass, not NMMO/water mixtures. Nevertheless, some control experiments with NMMO/water in the premix were carried out to make sure that the results were identical with employing only (anhydrous) NMMO. Since we were mainly interested in possible chemical side reactions in the systems, these simplifications were considered completely acceptable.

The most obvious outcome of the experiments involving biomass was that the chemical behaviour of the system GVL/NMMO/water changed totally. Generally, there was a considerable degradation of both NMMO and GVL already at the lowest temperature tested, as described below. Under some conditions, the system was even unstable and tended to uncontrollable reactions.

It is well known from the literature that NMMO tends towards spontaneous, uncontrollable reactions if transition metal ions, acylating or alkylating agents, or simply acids are present. This instability, which increases with higher temperature, is generally due to an activation of the N–O bond in the amine *N*-oxide. In the following, the autocatalytic degradation of NMMO is triggered, in which a degradation product of NMMO, the carbenium-iminium ion *N*-(methylene)morpholinium, induces NMMO degradation and is constantly regenerated in this process, resulting in uncontrollable degradation and processes that are euphemistically called “exothermic events”.^{4,5}

CAUTION! *It should be noted that exothermic reactions involving NMMO may proceed violently and may cause explosions and fire. This poses severe risks for health and wellbeing. Appropriate personal protection is imperative!* When studying the system GVL/NMMO/water biomass it was evident that in several cases the system became unstable, resulting in complete charring of the reaction mixtures without any compounds that could reasonably be retrieved. As the same reaction mixtures – without NMMO being present – were completely stable, it was evident that NMMO was the culprit in all those cases. In the charred residues of such reactions, NMMO was completely absent, GVL was present only in traces, and the biomass converted to a black viscous char or black solid. The addition of 3% propyl gallate (rel. to NMMO), which is commonly added to stabilize NMMO solutions in fibre making or biomass pro-

cessing, had no effect whatsoever, and the far-reaching degradation occurred no matter whether propyl gallate was present or not.

Fig. 2 shows under which compound ratios and conditions charring occurred (red) and which ones were safe (green). In general, the system became more stable with higher water contents, and this protective effect of water diminished with increasing reaction temperatures. At 100 °C, no charring occurred at all, at 125 °C only in GVL without water present, at 150 °C at GVL/water ratios of 100:0, 90:10 and at 180 °C under almost all conditions except GVL water ratios of 50:50 and 60:40. Furthermore, it was interesting to see that in the case of an uncontrollable reaction occurring, the content of NMMO made almost no difference with regard to the extent of charring. The formation of black remainders was as severe at 5% NMMO as it was at 15%. Apparently the exothermicity of the NMMO degradation was so severe that already small amounts affected the reaction mixture in its entirety.

The most important conclusion – because aspects of health and safety at work might be concerned – was that at 180 °C the water content in the GVL/NMMO/water system must not be lower than 40% to make sure that no uncontrollable exothermic events due to NMMO occur. At lower temperatures, water contents can be lowered without impairing the integrity of the system, about 25% at 150 °C and 10% at 125 °C. Without water in the GVL phase, the presence of NMMO and biomass is generally unsafe, even at a temperature as low as 100 °C. Concluding from these results, we excluded further experiments under conditions which had proven to be unstable and uncontrollable.

In Fig. 3, the consumption of GVL and NMMO in the quaternary system GVL/NMMO/water/biomass is summarized, with the numerical yield values listed in the ESI.† The figure is thus analogous to Fig. 1, which describes GVL/NMMO/water, *i.e.* the same system, but without biomass. It was evident that the presence of biomass changed the chemistry of the system fundamentally. While in the ternary system GVL/NMMO/water chemical reactions, and thus the extent of GVL or NMMO degradation, were quite limited, they became extensive in the presence of biomass. Since GVL as a solvent in organosolv processing is known to be more or less inert (apart from minor hydrolysis),⁴⁶ the chemical instability obviously had to be attributed to the NMMO (and later on its degradation products) which additionally entered the system.

At 100 °C, the system was able to consume roughly 10% of NMMO (rel. to biomass) at 100% GVL. Consequently, if 20% NMMO was contained, the consumption was approx. half of it. With higher water contents, the consumption of NMMO decreased, so that approx. 3–4% of NMMO (rel. to biomass) were consumed by the system (74% of the 5% NMMO charge or 18% of the 20% NMMO charge). The GVL degradation was minor. It reached a maximum of about 12% at 100% GVL, but already 10% of water decreased the GVL consumption to about 8% and 50% water to about 4%. It was interesting to note that, in a first approximation, 1% of degraded NMMO was able to trigger a GVL consumption of at least 4%, with this number

increasing to 12% with decreasing water contents. The reaction was thus by no means a stoichiometric process as in the biomass-free case discussed above (Fig. 1), but a complex system with multiple parallel and interlinked reactions.

Increasing the temperature to 125 °C generally intensified the degradation reactions as expectable. In water-free GVL the system is unstable (see Fig. 2). At all GVL/water ratios 5% NMMO was completely consumed, except GVL/water = 50:50 where consumption was “only” approx. 4.25% (85% of the 5%). At 90/10 GVL/water, 54% of the NMMO in the 20% batch were consumed, this value went down to 24% in the GVL/water = 50:50 batch. Roughly approximated, about 1.5 to 2 times more NMMO (if present in sufficient amounts) was consumed than in the analogous system at 100 °C. GVL consumption increased as well. In 90:10 GVL/water, up to approx. 15% of the solvent are lost in degradation reactions, in the batch containing 50% water only approx. 9%. The consumption of GVL at 125 °C was roughly 1.5 to 2 times higher than at 100 °C, the factor of increase thus being similar to that for NMMO consumption.

At 150 °C, a region is reached in which the chemical system is not stable anymore at GVL/water ratios of 100:0 and 90:10, undergoing uncontrollable degradation. 10% NMMO was completely consumed at all GVL/water ratios. At the highest NMMO charge of 20%, 94% of it were degraded at a GVL/water ratio of 80/20 and 64% at a GVL/water ratio of 50:50. With regard to GVL consumption the system became different insofar as the GVL/water ratio lost its influence and the GVL consumption was rather constant at a high level. At 5% NMMO (rel. to biomass), approx. 11% of GVL was lost, 17% at a 10% NMMO charge, 22% at 15% NMMO, and 26% at 20% NMMO. The lower values at 5 and 10% NMMO are due to the fact that the system cannot convert more NMMO than present, NMMO being the “limiting factor”. GVL consumption at 20% NMMO and at a 50:50 GVL/water ratio was 30%, and thus increased more than threefold relative to the 125 °C system.

180 °C is the typical temperature for organosolv biomass separation with GVL. This temperature is largely incompatible with the presence of NMMO. Only at GVL/water ratios of 50:50 and 60:40 NMMO was tolerated, at all other ratios and lower water contents the system became unstable and exothermicities with complete product charring occurred. But even at those two “innocent” GVL/water ratios, the NMMO in the system was entirely degraded. NMMO, at this typical biomass processing temperature of GVL, would thus not have any beneficial effect as it is fast and quantitatively consumed. The consumption of GVL was pronounced as well and, as expected, considerably higher than at 150 °C. At 5% NMMO (rel. to biomass), 9% of the GVL was lost, *i.e.* approximately the same mass as the biomass contained and 18 times more (molar ratio) than the contained NMMO. At a 20% NMMO charge (rel. to biomass), GVL consumption was as high as 35%, 3.5 times the weight of the biomass and again about 18 times more than the NMMO in the system. Thus, also from the viewpoint of GVL loss and recovery, the combination of GVL with NMMO would have to be considered unreasonable.

Although the system GVL/NMMO/water/biomass was described successfully with regard to the net degradation processes, we were hoping to be able to specify the degradation processes in more detail. It was evident that the interaction between NMMO and biomass caused the decomposition reactions in the system (in combination with GVL; neither NMMO alone nor biomass alone would cause similar processes).

However, due to simplification, “biomass” had so far been considered only as one component with overall reactivity. In a further set of experiments we therefore replaced the beech sawdust used before with the same mass of either pure cellulose, a beech milled wood lignin or isolated beech xylan, respectively, as well as a mixture thereof.

Exemplary conditions used 10% of biomass (or biomass component), 10% of NMMO relative to the biomass, a GVL/water ratio of 80 : 20 or 60 : 40 at temperatures of either 150 or 180 °C. The results are shown in Fig. 4. At 180 °C and a GVL/water ratio of 80 : 20, the system was unstable and reacted in an uncontrolled way in the case of biomass, lignin, and simulated biomass (cellulose/lignin/xylan = 1 : 1 : 1 by weight), whereas it remained stable in the case of cellulose and xylan, although pronounced NMMO and GVL consumption occurred also then. At 180 °C and a GVL/water ratio of 60 : 40, as well as at 150 °C and both GVL/water ratios, degradation reactions were obvious, which however took no violent course (Fig. 4).

It was obvious that cellulose was the most innocent component in the biomass, causing nearly no side reactions beyond the minor processes observed in the biomass-free system (*cf.* Fig. 1 and Scheme 1). Compared to biomass as a whole, cellulose effected only roughly one tenth of the GVL and NMMO degradation processes. Analysis of the cellulose – after 2 h in a 60 : 40 mixture of GVL/NMMO at 180 °C – by gel permeation chromatography⁴⁸ with group-selective profiling of carbonyl groups (CCOA method)⁴⁹ and carboxyl groups (FDAM method)⁵⁰ showed a minor chain degradation and an increase in carbonyl content (from 8 to about 13.5 $\mu\text{mol g}^{-1}$) besides a conversion of the celluloses reducing end groups into carboxylic acids (2 to 12 $\mu\text{mol g}^{-1}$). This cellulose oxidation went parallel with the reduction of NMMO into NMM. This behaviour of cellulose towards NMMO is well known from Lyocell systems, *i.e.* solutions of cellulose in NMMO monohydrate, and from the chemistry of these systems.^{4,5}

The reactivity of xylan was higher than that of cellulose, and caused about three times higher GVL consumption and about twice higher NMMO degradation. It showed about a quarter of the reactivity of the whole biomass, measured in terms of GVL and NMMO consumption. The strong discoloration of the mixture was indicative of condensation reactions of primary furanoid products easily derived from xyans.⁵⁰ Furfural, as the primary thermal dehydration product of xylose, is oxidized by NMMO to 2-furancarboxylic acid which undergoes further condensation to potent chromophores. The reactions of primary xylan degradation products with NMMO, also known from lyocell chemistry,⁴ also explain the higher NMMO consumption than in the cellulose case.

Lignin had by far the most pronounced effect on the instability of the GVL/NMMO system, showing a reactivity about 3–4 times higher than biomass as a whole, measured in terms of NMMO and GVL degradation. While NMMO was completely degraded in all cases, GVL consumption approached 70%. This effect is primarily due to phenolic lignin structures which are readily oxidized by NMMO at the elevated temperatures.⁴ The generated NMM on the one hand promotes GVL hydrolysis and on the other hand deprotonates lignin phenols to the phenolates which in turn – as potent nucleophiles – consume GVL by transesterification. These two NMM-promoted processes both contribute to GVL consumption. The fact that the redox process between NMMO and the lignins phenolic structures was the trigger of the side reaction was nicely proven by the application of lignin in which the phenolic OH groups were blocked by permethylation: under the same conditions (2 h in a 60 : 40 mixture of GVL/NMMO at 180 °C) the consumption of NMMO and GVL was less than 10% and 3%, respectively. Model compounds confirmed the polymer case: methoxy-hydroquinone, a lignin model compound, had the same effect as its parent polymer (a GVL consumption of 70% and complete NMMO loss), while the corresponding permethylated model compound, *i.e.* 1,2,4-trimethoxybenzene, behaved nearly inert with 3% GVL loss and 12% NMMO degradation. The readily oxidizable structures in the lignin are thus the crucial structural elements responsible for NMMO consumption and – as a direct consequence – for GVL loss.

Assuming a rough compositional ratio of cellulose/lignin/xylan of 1 : 1 : 1 in the used biomass, the observed behavior of the system with biomass results quite well from the additive reactivities of the three individual components (“model mix” in Fig. 4). The simulated biomass mixture of one third cellulose, one third lignin and one third xylan behaved very similarly to the original biomass, which confirmed the observed reactivity gradation of cellulose < xylan << biomass << lignin. More details on the analysis of the biomass and biomass components after treatment in the NMMO/GVL/water system will be presented in a follow-up report.

Identification of GVL-derived and NMMO-derived degradation products in the system GVL/NMMO/water/biomass

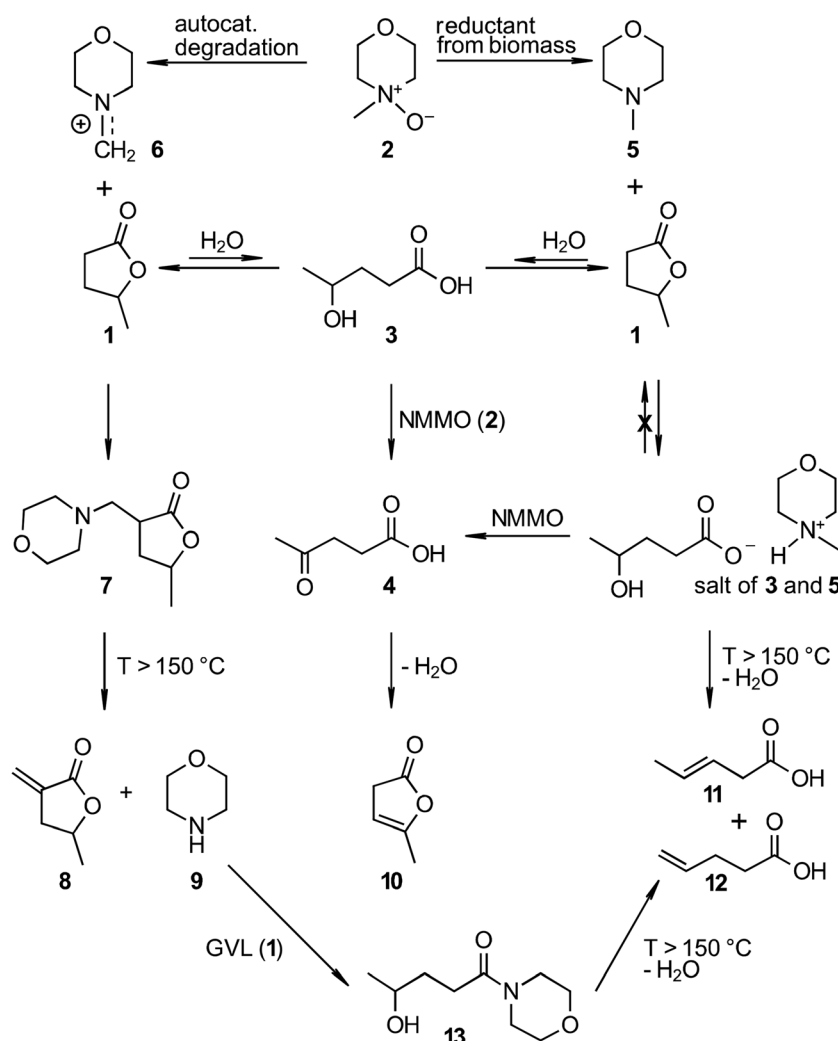
Even more pressing than in the case of the GVL/NMMO/water system with its relatively insignificant by-product generation, the question of the nature of the degradation products became of central interest when biomass was involved. In addition, the issue of identification of these by-products was scientifically quite demanding. The biomass component now being present in the system (GVL/NMMO/water/biomass) – with its multitude of components and structures contained – introduced a factor of huge complexity. While at 100 °C and at 125 °C chemical biomass modification was less prominent, it became pronounced at 150 °C and even more at 180 °C. The fractionating effect of GVL, the basis of organosolv separation of biomass components, as well as the oxidizing effect of NMMO and the interaction of both components came together to generate a

“black liquor sludge” mixture of utter complexity. While measuring the consumption of GVL or NMMO was relatively easy (*cf.* Fig. 1–3), the determination of the reaction products was much more intricate, and a reliable quantification turned out to be virtually impossible.

In the following, we therefore report on the main degradation products of GVL and NMMO, which amount to approx. 80–85% of the consumed GVL and NMMO. The residual 15–20% could not be reliably identified as the number of individual compounds was too high or they were (physically or covalently) bound to the biomass components. In general, the biomass components were precipitated by water addition at r.t., different pH ranges were set and the degradation products extracted by organic solvents. Possible minor reactions that occurred during this room temperature process were assumed to be negligible, although they cannot be ruled out completely. The main reactions proceeding in the system GVL/NMMO/water/biomass and the main degradation products of GVL and NMMO are summarized in Scheme 2.

All compounds were comprehensively characterized (see the Experimental section) and the structure was additionally confirmed by comparison with authentic samples, which were either independently synthesized or commercially available.

The formation of the degradation products can be best categorized according to the reaction temperature since several products were only formed above a certain temperature. This is attempted in Table 1, which shows the prominence of the degradation products at the respective reaction temperatures. There was no dependence on the NMMO content, *i.e.*, all degradation products that were found at higher NMMO concentrations were also present at a lower NMMO content, only in smaller concentrations. The water content had a noticeable, but minor, influence on the ratio of the degradation products. Higher water contents favoured the degradation pathways involving the primary hydrolysis product of GVL, *i.e.* 4-hydroxyvaleric acid (3) and the products of its follow-up chemistry. At the same time, deoxygenation of NMMO to *N*-methylmorpholine (5) was slightly favoured, and the alterna-



Scheme 2 Degradation products of GVL (1) and NMMO (2) formed in the system GVL/NMMO/water/biomass and their main formation and conversion reactions.

Table 1 Dependence of degradation product formation on the reaction temperature

Degradation products	100 °C	125 °C	150 °C	180 °C
4-Hydroxyvaleric acid (3)	2–5	17–19	36–42	16–18
Levulinic acid (4)		1–3	3–4	
<i>N</i> -Methylmorpholine (5)	20–25	52–60	68–72	79–83
α -Morpholinomethyl-GVL (7)		<1	12–15	
α -Methylene-GVL (8)			<1	9–13
Morpholine (9)		<1	<1	
α -Angelicalactone (10)		2–3	2–4	
3-Pentenoic acid (11)				15
4-Pentenoic acid (12)				17–18
4-Hydroxyvaleric acid morpholide (13)			3–4	8–10

Yield ranges are given in % relative to NMMO (in normal font) or relative to GVL (in italic font). Empty cells: not detected.

tive degradation path involving *N*-(methylene)morpholinium cations (6) somewhat disfavoured (see Scheme 2). All these effects were minor, however, compared to the large and dominating influence of reaction temperature on the by-product concentration and ratio as shown in Table 1. It should be noted that in the reaction mixture the acids present – either generated acids, such as 4-hydroxyvaleric acid and levulinic acid, or acidic functionalities present in biomass – form salts with the bases present (such as *N*-methylmorpholine or morpholine), whereas in the extracts used for identification these compounds are present in isolated form.

At 100 °C, the by-product formation is limited to the reaction of the oxidant NMMO with reducing functional groups in biomass, such as reducing ends of polysaccharides and phenols in lignin. This regenerates *N*-methylmorpholine (5) as the product of NMMO reduction, which in turn promotes hydrolysis of GVL.

While in pure water the equilibrium between open-chain 4-hydroxyvaleric acid (3) and GVL (1) is far on the side of the GVL ring structure,⁴⁷ the presence of a base, such as NMM, shifts this equilibrium by converting the acid into its salt form. Other side reactions of GVL and NMMO were not observed for the system at 100 °C so that 3 and 5 (2–5% rel. to GVL and 20–25% rel. to NMMO) were the only degradation products identified (Table 1).

At 125 °C, the oxidative power of NMMO is significantly increased and thus more NMM (5) is formed (52–60% rel. to NMMO), which in turn significantly increased the amount of 4-hydroxyvaleric acid (3) (17–19% rel. to GVL), being present as NMM salt and thus in a form that cannot react back to GVL. In addition, 4-hydroxyvaleric acid (3) is oxidized to levulinic acid (4) (1–3% rel. to GVL) by NMMO. At the increased reaction temperature, also the alternative degradation pathway of NMMO, involving *N*-(methylene)morpholinium cations (6) sets in, see Scheme 2. Inducible by many reagents, such as alkylating agents, acylating agent, acids or transition metal ions, this pathway can cause autocatalytic degradation of NMMO and the related exothermicities. This is the reason for the instability of the system at higher temperatures, when consumption of the *N*-(methylene)morpholinium cations by side reactions

cannot compensate anymore for their generation. At 125 °C, the amount of these carbenium-iminium ions is relatively small, and uncontrollable reactions occurred only in 100% (water-free) GVL. The *N*-(methylene)morpholinium cations reacted with GVL as the most prominent compound present in α -morpholinomethyl- γ -valerolactone (7) (less than 1% rel. to NMMO), *i.e.*, an aminomethylation occurred at the weakly CH-acidic (methylene-active) α -position to the lactone carbonyl function. This is a good example of a degradation product that combines both NMMO and GVL moieties in one molecule and thus unambiguously evidences their involvement in mutual side reactions. Another process setting in with the elevated temperature was the cyclization of levulinic acid (4) to 5-methylfuran-2(3*H*)-one (10), also called α -angelicalactone, which can be conceived as the intramolecular ester (lactone) of the *endo*-enol form of levulinic acid (1–2% rel. to GVL). It is distinguished from GVL by a C3–C4 double bond. Noticeably, 10 is not formed from GVL directly by oxidation (GVL is inert towards NMMO, see above), but by the “detour” pathway *via* 4-hydroxyvaleric acid (3), which is oxidized to levulinic acid (4) and subsequently dehydrated to the unsaturated lactone 10.

At 150 °C, with the conditions becoming more drastic and exceeding the temperatures of max. 130 °C at which NMMO is usually applied, the chemistry of the system changed in a way that degradation became significantly more pronounced. With only small amounts of water present (GVL/water = 100 : 0 or 90 : 10) the autocatalytic degradation of NMMO dominates and the system is thus unstable. At higher water contents, NMMO reduction is more pronounced, and so is the generation of 4-hydroxyvalerate by NMM-catalyzed GVL hydrolysis. NMM (5) and 4-hydroxyvaleric acid (3) are the dominating products (up to 72% and up to 42% degradation rel. to NMMO and GVL, respectively), but also α -morpholinomethyl- γ -valerolactone (7), resulting from the alternative NMMO degradation pathway, becomes more prominent than at 125 °C (15% rel. to NMMO). Some traces of free morpholine (9) were found, which in the presence of water is in equilibrium with *N*-(methylene)morpholinium cations, as well as its aminolysis product with GVL, 4-hydroxyvaleric acid morpholide (13) (3–4% rel. to NMMO). This amide is formed from GVL and morpholine at temperatures above 130 °C in a direct, non-catalyzed reaction. Formation of levulinic acid (4) and its cyclization product α -angelicalactone (10) was not significantly more pronounced than at 125 °C, see Table 1.

At a temperature of 180 °C, the by-product chemistry of the system changes once more. At water contents lower than 30% (relative to GVL), the system becomes unstable in a way that exothermicities with complete charring and loss of the chemicals occur. Also, at higher water contents, NMMO is completely consumed in all cases, being converted mainly into NMM (5) (79–83% rel. to NMMO). Morpholine as the second NMMO-degradation product is not found as a free compound, but in the form of the GVL-aminolysis product 4-hydroxyvaleric acid morpholide (13) (12–15% rel. to NMMO), which becomes more prominent than at 150 °C. α -Morpholinomethyl-GVL (7), a major product at 150 °C, is not detected anymore, but its

thermal elimination product α -methylene-GVL (8) (9–13% rel. to NMMO), formed from 7 by loss of morpholine – which in turn reacts with GVL to 4-hydroxyvaleric acid morpholide (13). At the high temperature, also the 4-hydroxyvalerate salts are not stable, but eliminate water – likely catalysed by the bases present (NMM or morpholine) – to form 3-pentenoic acid (11) and 4-pentenoic acid (12) (15% and 17–18% rel. to GVL, respectively). Both unsaturated acids, present in *trans*-configuration, were only found at 180 °C. They must have formed from the salt forms of 4-hydroxyvaleric acid (3), because the free acid would undergo immediate cyclization to GVL rather than elimination. The amines in the system thus have a double function in this reaction, by acting as a base for initial salt formation and as a subsequent elimination catalyst.

Conclusions

In summary, the combination of NMMO pretreatment and subsequent GVL biomass fractionation is not recommendable, unless complete removal of NMMO after the pretreatment step can be guaranteed. Even at temperatures as low as 100 °C, both NMMO and GVL undergo side reactions and are thus lost at least partly. At higher temperatures, the system becomes increasingly unstable at lower water contents so that uncontrollable reactions might occur that might endanger equipment and workers. These processes are caused by the highly exothermic autocatalytic degradation of NMMO. At temperatures relevant for biomass separation with GVL/water, all the NMMO contained is completely lost, but also considerable amounts of GVL are consumed. The losses in GVL in a molar ratio are up to 18 times higher than the contained NMMO: 2% of NMMO (relative to GVL, 20% relative to biomass) causes a loss of more than one third (36%) of the GVL by side reactions. This is mainly due to the catalytic action of the amines (*N*-methylmorpholine and morpholine) formed from NMMO.

Degradation reactions in the system are initiated by the redox reaction of NMMO – acting as the oxidant and being converted into NMM – with the biomass, followed a complex system of degradation reactions. Lignin was roughly 3–4 times more redox-reactive, due to its readily oxidizable phenolic structures, than the biomass as a whole, expressed as the extent of by-product formation in the GVL/NMMO/water system. Xylan and cellulose behaved largely inert and experienced only minor oxidation as seen by group-selective fluorescence labeling. With increasing temperature the oxidative power of NMMO increases: both oxidation and thermal elimination processes of primary GVL degradation products become more dominant. About 75% of the degradation products of GVL and NMMO could be identified in this study, and their formation chemistry explained.

Conflicts of interest

There are no conflicts to declare.

Acknowledgements

The support by the Austrian Biorefinery Center Tulln (ABCT) is gratefully acknowledged.

References

- 1 G. Meister and M. Wechsler, *Biodegradation*, 1998, **9**, 91–102.
- 2 (a) H. Firgo, M. Eibl and D. Eichinger, *Lenzinger Ber.*, 1996, **75**, 47–50; (b) I. Marini and F. Brauneis, *Textilveredlung*, 1996, **31**, 182–186.
- 3 E. Linton, *J. Am. Chem. Soc.*, 1940, **62**, 1945–1948.
- 4 T. Rosenau, A. Potthast, H. Sixta and P. Kosma, *Prog. Polym. Sci.*, 2001, **26**, 1763–1837.
- 5 T. Rosenau, A. Potthast, P. Kosma, C.-L. Chen and J. S. Gratzl, *J. Org. Chem.*, 1999, **64**, 2166–2167.
- 6 (a) T. Rosenau, P. Schmid, A. Potthast and P. Kosma, *Holzforschung*, 2005, **59**, 503–506; (b) T. Rosenau, A. Potthast, I. Adorjan, A. Hofinger, H. Sixta, H. Firgo and P. Kosma, *Cellulose*, 2002, **9**, 283–291.
- 7 A. Albini, *Synthesis*, 1993, 263–277.
- 8 A. G. Godfrey and B. Ganem, *Tetrahedron Lett.*, 1990, **31**, 4825–4826.
- 9 B. Dasgupta and W. A. Donaldson, *Tetrahedron Lett.*, 1998, **39**, 343–346.
- 10 (a) T. Rosenau, A. Potthast, T. Elder and P. Kosma, *Org. Lett.*, 2002, **4**(24), 4285–4288; (b) T. Rosenau, A. Hofinger, A. Potthast and P. Kosma, *Org. Lett.*, 2004, **6**, 541–544.
- 11 S. Yokota, T. Kitaoka, M. Opietnik, T. Rosenau and H. Wariishi, *Angew. Chem., Int. Ed.*, 2008, **47**, 9866–9869.
- 12 C.-H. Kuo and C.-K. Lee, *Carbohydr. Polym.*, 2009, **77**, 41–46.
- 13 C.-H. Kuo and C.-K. Lee, *Bioresour. Technol.*, 2009, **100**, 866–871.
- 14 H. P. Fink, P. Weigel, H. J. Purz and J. Ganster, *Prog. Polym. Sci.*, 2001, **26**, 1473–1524.
- 15 (a) L.-Y. Cai, Y.-L. Ma, X.-X. Ma and J.-M. Lv, *Bioresour. Technol.*, 2016, **212**, 42–46; (b) R. Wikandari, R. Millati and M. J. Taherzadeh, in *Biomass Fractionation Technologies for a Lignocellulosic Feedstock Based Biorefinery*, ed. S. I. Mussatto, Elsevier, Amsterdam, 2016, pp. 255–280; (c) S. Sen, J. D. Martin and D. S. Argyropoulos, *ACS Sustainable Chem. Eng.*, 2013, **1**, 858–870; (d) M. Shafiei, K. Karimi and M. J. Taherzadeh, *Bioresour. Technol.*, 2010, **101**, 4914–4918.
- 16 (a) Y.-C. He, D.-Q. Xia, C.-L. Ma, L. Gong, T. Gong, M.-X. Wu, Y. Zhang, Y.-J. Tang, J.-H. Xu and Y.-Y. Liu, *Bioresour. Technol.*, 2013, **135**, 18–22; (b) M. Khodaverdi, A. Jeihanipour, K. Karimi and M. J. Taherzadeh, *J. Ind. Microbiol. Biotechnol.*, 2012, **39**, 429–438; (c) Y. Liu, Q. Zhong, S. Wang and Z. Cai, *Biomacromolecules*, 2011, **12**, 2626–2632.
- 17 M. J. Taherzadeh and K. Karimi, *Int. J. Mol. Sci.*, 2008, **9**, 1621–1651.

- 18 C. Cuissinat and P. Navard, *Macromol. Symp.*, 2006, **244**, 1–18.
- 19 (a) F. A. Purwandari, A. P. Sanjaya, R. Millati, M. N. Cahyanto, I. S. Horváth, C. Niklasson and M. J. Taherzadeh, *Bioresour. Technol.*, 2013, **128**, 461–466; (b) A. Teghammar, K. Karimi, I. S. Horvath and M. J. Taherzadeh, *Biomass Bioenergy*, 2012, **36**, 116–120.
- 20 P. R. Lennartsson, C. Niklasson and M. J. Taherzadeh, *Bioresour. Technol.*, 2011, **102**, 4425–4432.
- 21 (a) S. Aslanzadeh, A. Berg, M. J. Taherzadeh and I. S. Horvath, *Appl. Biochem. Biotechnol.*, 2014, **172**, 2998–3008; (b) M. Shafiei, K. Karimi, H. Zilouei and M. J. Taherzadeh, *BioMed Res. Int.*, 2014, **2014**, 469378; (c) A. Goshadrou, K. Karimi and M. J. Taherzadeh, *Biomass Bioenergy*, 2013, **49**, 95–101.
- 22 (a) N. Poornejad, K. Karimi and T. Behzad, *Ind. Crops Prod.*, 2013, **41**, 408–413; (b) S. Ramakrishnan, J. Collier, R. Oyetunji, B. Stutts and R. Burnett, *Bioresour. Technol.*, 2010, **101**, 4965–4970; (c) J. Kubikova, P. Lu, A. Zemann, P. Krkoska and O. Bobleter, *Cellul. Chem. Technol.*, 2000, **34**, 151–162.
- 23 Sigma-Aldrich: γ -Valerolactone. <https://www.sigmaaldrich.com/catalog/product/aldrich/w310311?lang=de®ion=AT> Accessed 17/12/2020.
- 24 T. Adams, D. Greer, R. Ford, J. Doull, I. Munro, P. Newberne, P. S. Portoghese, R. L. Smith, B. M. Wagner, C. S. Weil, L. A. Woods and R. A. Ford, *Food Chem. Toxicol.*, 1998, **36**, 249–278.
- 25 A. P. Dunlop and J. W. Madden, US2786852A, 1957.
- 26 S. Tanaka, K. Fukuda and T. Asada, US7491833B2, 2009.
- 27 (a) S. G. Wettstein, J. Q. Bond, D. M. Alonso, H. N. Pham, A. K. Datye and J. A. Dumesic, *Appl. Catal., B*, 2012, **117–118**, 321–329; (b) W. R. H. Wright and R. Palkovits, *ChemSusChem*, 2012, **5**, 1657–1667; (c) D. J. Braden, C. A. Henao, J. Heltzel, C. C. Maravelias and J. A. Dumesic, *Green Chem.*, 2011, **13**, 1755–1765; (d) P. P. Upare, J.-M. Lee, D. W. Hwang, S. B. Halligudi, Y. K. Hwang and J.-S. Chang, *J. Ind. Eng. Chem.*, 2011, **17**, 287–292; (e) L. E. Manzer, US6617464B2, 2003; (f) R. V. Christian Jr., H. D. Brown and R. Hixon, *J. Am. Chem. Soc.*, 1947, **69**, 1961–1963.
- 28 (a) I. T. Horváth, *Green Chem.*, 2008, **10**, 1024–1028; (b) I. T. Horváth, H. Mehdi, V. Fábos, L. Boda and L. T. Mika, *Green Chem.*, 2008, **10**, 238–242.
- 29 I. Horváth, H. Mehdi, V. Fábos and L. Boda, in *234th ACS National Meeting*, 2007.
- 30 L. Qi and I. T. Horváth, *ACS Catal.*, 2012, **2**, 2247–2249.
- 31 D. M. Alonso, J. M. R. Gallo, M. A. Mellmer, S. G. Wettstein and J. A. Dumesic, *Catal. Sci. Technol.*, 2013, **3**, 927–931.
- 32 D. M. Alonso, S. G. Wettstein, M. A. Mellmer, E. I. Gurbuz and J. A. Dumesic, *Energy Environ. Sci.*, 2013, **6**, 76–80.
- 33 (a) A. H. Motagamwala, W. Won, C. T. Maravelias and J. A. Dumesic, *Green Chem.*, 2016, **18**, 5756–5763; (b) J. S. Luterbacher, A. Azarpira, A. H. Motagamwala, F. Lu, J. Ralph and J. A. Dumesic, *Energy Environ. Sci.*, 2015, **8**, 2657–2663; (c) M. A. Mellmer, D. M. Alonso, J. S. Luterbacher, J. M. R. Gallo and J. A. Dumesic, *Green Chem.*, 2014, **16**, 4659–4662; (d) L. Qi, Y. F. Mui, S. W. Lo, M. Y. Lui, G. R. Akien and I. T. Horváth, *ACS Catal.*, 2014, **4**, 1470–1477.
- 34 (a) F. Huang, W. Li, Q. Liu, T. Zhang, S. An, D. Li and X. Zhu, *Fuel Process. Technol.*, 2018, **181**, 294–303; (b) Y. Rodenas, R. Mariscal, J. Fierro, D. M. Alonso, J. Dumesic and M. L. Granados, *Green Chem.*, 2018, **20**, 2845–2856; (c) C. Sener, A. H. Motagamwala, D. M. Alonso and J. A. Dumesic, *ChemSusChem*, 2018, **11**, 2321–2331; (d) B. Song, Y. Yu and H. Wu, *Fuel*, 2018, **232**, 317–322; (e) X. Li, Q. Liu, C. Luo, X. Gu, L. Lu and X. Lu, *ACS Sustainable Chem. Eng.*, 2017, **5**, 8587–8593; (f) Q. Qing, Q. Guo, L. Zhou, Y. Wan, Y. Xu, H. Ji, X. Gao and Y. Zhang, *Bioresour. Technol.*, 2017, **226**, 247–254; (g) A. Ghosh, R. C. Brown and X. Bai, *Green Chem.*, 2016, **18**, 1023–1031; hW. Li, Z. Xu, T. Zhang, G. Li, H. Jameel, H.-m. Chang and L. Ma, *BioResources*, 2016, **11**, 5839–5853.
- 35 E. I. Gürbüz, J. M. R. Gallo, D. M. Alonso, S. G. Wettstein, W. Y. Lim and J. A. Dumesic, *Angew. Chem., Int. Ed.*, 2013, **52**, 1270–1274.
- 36 (a) L. Jia, Y. Qin, J. Wang and J. Zhang, *Bioresour. Technol.*, 2020, **302**, 122901; (b) Q. Qing, X. Gao, P. Wang, Q. Guo, Z. Xu and L. Wang, *RSC Adv.*, 2018, **8**, 17527–17534; (c) R. M. Trevorah, T. Huynh, T. Vancov and M. Z. Othman, *Bioresour. Technol.*, 2018, **250**, 673–682; (d) X. Kong, H. Xu, H. Wu, C. Wang, A. He, J. Ma, X. Ren, H. Jia, C. Wei, M. Jiang and P. Ouyang, *Process Biochem.*, 2016, **51**, 1538–1543; (e) L. Shuai, Y. M. Questell-Santiago and J. S. Luterbacher, *Green Chem.*, 2016, **18**, 937–943; (f) M. Wu, Z. Y. Yan, X. M. Zhang, F. Xu and R. C. Sun, *Bioresour. Technol.*, 2016, **200**, 23–28.
- 37 (a) H. Q. Lê, K. Dimic-Misic, L.-S. Johansson, T. Maloney and H. Sixta, *Cellulose*, 2018, **25**, 179–194; (b) H. Q. Lê, J.-P. Pokki, M. Borrega, P. Uusi-Kyyny, V. Alopaeus and H. Sixta, *Ind. Eng. Chem. Res.*, 2018, **57**, 15147–15158; (c) H. Q. Lê, Y. Ma, M. Borrega and H. Sixta, *Green Chem.*, 2016, **18**, 5466–5476; (d) W. Fang and H. Sixta, *ChemSusChem*, 2015, **8**, 73–76.
- 38 D. M. Alonso, S. H. Hakim, S. Zhou, W. Won, O. Hosseinaei, J. Tao, V. Garcia-Negron, A. H. Motagamwala, M. A. Mellmer, K. Huang, C. J. Houtman, N. Labbé, D. P. Harper, C. T. Maravelias, T. Runge and J. A. Dumesic, *Sci. Adv.*, 2017, **3**, e1603301.
- 39 L. Shuai, M. T. Amiri, Y. M. Questell-Santiago, F. Héroguel, Y. Li, H. Kim, R. Meilan, C. Chapple, J. Ralph and J. S. Luterbacher, *Science*, 2016, **354**, 329–333.
- 40 (a) B. Satari, K. Karimi and R. Kumar, *Sustainable Energy Fuels*, 2019, **3**, 11–62; (b) E. C. Bensah and M. Mensah, *Int. J. Chem. Eng.*, 2013, **2013**, 719607; (c) G. Brodeur, J. Telotte, J. J. Stickel and S. Ramakrishnan, *Bioresour. Technol.*, 2016, **220**, 621–628.
- 41 (a) N. Pircher, L. Carbajal, C. Schimper, M. Bacher, H. Rennhofer, J.-M. Nedelec, H. C. Lichtenegger, T. Rosenau and F. Liebner, *Cellulose*, 2016, **23**, 1949–1966; (b) S. Chrapava, D. Touraud, T. Rosenau, A. Potthast and W. Kunz, *Phys. Chem. Chem. Phys.*, 2003, **5**, 1842–1847.

- 42 U. Henniges, E. Kloser, A. Patel, A. Potthast, P. Kosma, M. Fischer, K. Fischer and T. Rosenau, *Cellulose*, 2007, **14**, 497–511.
- 43 (a) P. Korntner, T. Hosoya, T. Dietz, K. Eibinger, H. Reiter, M. Spitzbart, T. Röder, A. Borgards, W. Kreiner, A. K. Mahler, H. Winter, Y. Groiss, A. D. French, U. Henniges, A. Potthast and T. Rosenau, *Cellulose*, 2015, **22**, 1053–1062; (b) T. Rosenau, A. Potthast, K. Krainz, Y. Yoneda, T. Dietz, Z. P.-I. Shields and A. D. French, *Cellulose*, 2011, **18**, 1623–1633.
- 44 (a) G. Ebner, S. Schiehser, A. Potthast and T. Rosenau, *Tetrahedron Lett.*, 2008, **49**, 7322–7324; (b) F. Liebner, G. Ebner, E. Becker, A. Potthast and T. Rosenau, *Holzforschung*, 2010, **64**, 161–166.
- 45 (a) M. Balakshin, E. A. Capanema, X. Zhu, I. Sulaeva, A. Potthast, T. Rosenau and O. J. Rojas, *Green Chem.*, 2020, **22**, 3985–4001; (b) H. Amer, T. Nypelö, I. Sulaeva, M. Bacher, U. Henniges, A. Potthast and T. Rosenau, *Biomacromolecules*, 2016, **17**, 2972–2980.
- 46 (a) M. Becker, F. Liebner, T. Rosenau and A. Potthast, *Talanta*, 2013, **115**, 642–651; (b) A. Bogolitsyna, M. Becker, A. Borgards, F. Liebner, T. Rosenau and A. Potthast, *Holzforschung*, 2012, **66**, 917–925.
- 47 C. Y. Y. Wong, A. W.-T. Choi, M. Y. Lui, B. Fridrich, A. K. Horváth, L. T. Mika and I. T. Horváth, *Struct. Chem.*, 2017, **28**, 423–429.
- 48 A. Potthast, T. Rosenau, U. Henniges, S. Schiehser, P. Kosma, B. Saake, S. Lebiada, S. Radosta, W. Vorwerk, H. Wetzler, A. Koschella, T. Heinze, G. Strobin, H. Sixta, M. Strlic and A. Isogai, *Cellulose*, 2015, **22**(3), 1591–1613.
- 49 (a) J. Röhring, A. Potthast, T. Rosenau, T. Lange, G. Ebner, H. Sixta and P. Kosma, *Biomacromolecules*, 2002, **3**, 959–968; (b) A. Potthast, J. Röhring, T. Rosenau, A. Borgards, H. Sixta and P. Kosma, *Biomacromolecules*, 2003, **4**(3), 743–749.
- 50 (a) R. Bohrn, A. Potthast, S. Schiehser, T. Rosenau, H. Sixta and P. Kosma, *Biomacromolecules*, 2006, **7**, 1743–1750; (b) T. Rosenau, A. Potthast, N. Zwirchmayr, T. Hosoya, H. Hettegger, M. Bacher, K. Krainz, Y. Yoneda and T. Dietz, *Cellulose*, 2017, **24**(9), 3703–3723; (c) T. Rosenau, A. Potthast, N. Zwirchmayr, H. Hettegger, F. Plasser, T. Hosoya, M. Bacher, K. Krainz, Y. Yoneda and T. Dietz, *Cellulose*, 2017, **24**(9), 3671–3687.